

Can heat exchangers excite vibrations?

- Thermoacoustic Instabilities as a Cause of Increased Pulsations
Within Gas Pressure Regulation and Measurement Plants -

1. Overview

A multitude of investigations performed on the vibration behavior of gas pressure regulation and measurement plants (GPRM plants) by KÖTTER Consulting Engineers (KCE) in the last ten years have yielded a whole range of results. Gas vibrations were observed time and again in heat exchangers which were optically and acoustically perceived as pipe vibrations by onlookers. This generally only poses a risk to the plant's safety if the gas vibration frequency and the pipe's natural frequency coincide from a structural and mechanical point of view. In such cases, resonant increases in vibrations occur that may well lead to damage [1].

The typical design of a gas pressure regulation plant consists of one or more operating and standby pipelines. Prior to reducing the pressure, the natural gas is generally heated by the heat exchanger in order to avoid dropping below the dewpoint as a result of the decrease in pressure and the inevitable Joule-Thomson effect. The gas properties, the pipeline geometry, and the site and type of the actual excitation source are also relevant to the occurrence of gas vibrations, also known as pressure pulsations.

During the course of previous measurements, increasing gas vibrations were observed between the regulator of the operating pipeline (in use) and the regulator of the neighboring standby pipeline (not in use). This is represented below using measurement results from an investigation.

The phenomenon of acoustic resonance and the associated pipe vibrations and the influence of the upstream flow measurement have been known for some time. Up to now it has been unclear why increased pressure pulsations occur in dependence on local gas heat-up and vary in intensity with the amount of heat supplied. After all of the available data has been analyzed, this phenomenon has now been attributed to a thermoacoustic instability. The local heat input in the heat exchanger leads to a pressure pulsation which in turn creates acoustic resonance on account of the reflections in the remaining pipe system, for example in the pressure regulator.

The principle of this thermoacoustic effect is presented on the basis of an experiment adapted to the problem. The thermoacoustic effect is then analyzed in more detail from a theoretical perspective with a view to excitation of acoustic resonances in a gas pressure regulation plant. Finally, reduction measures on the basis of the processed results are presented both for the planning phase of new plants and for existing plants.

2. Acoustic basics

A distinguishing feature of various acoustic waves is their propagation direction within the pipeline. Both longitudinal and transverse propagation directions are possible within the pipeline

(

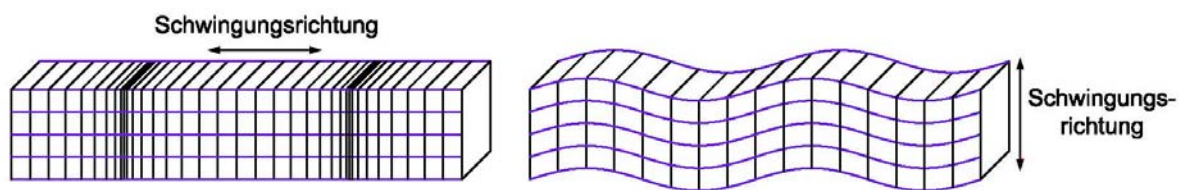


Figure 1: Acoustic wave propagation - longitudinal and transverse

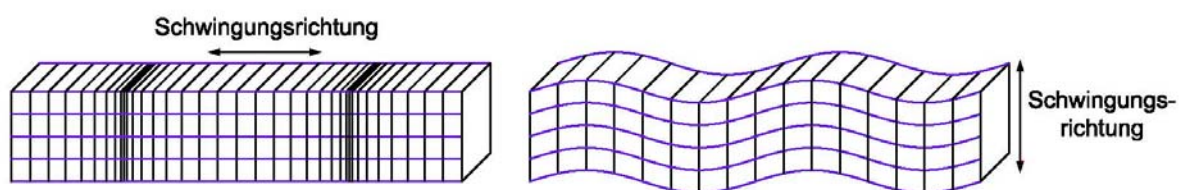


Figure 1: Acoustic wave propagation - longitudinal and transverse

The propagating waves are reflected by, for example, mountings or surrounds. By superimposing incoming and reflected waves, both plane waves and diametrical or annular modes may develop (see Figure 2: Graphical representation of the reinforcement mechanism of acoustic resonances in pipelines.). Within these transverse modes, a distinction can be made between the number of radial (n) nodal lines and the nodal lines distributed around the circumference (m).

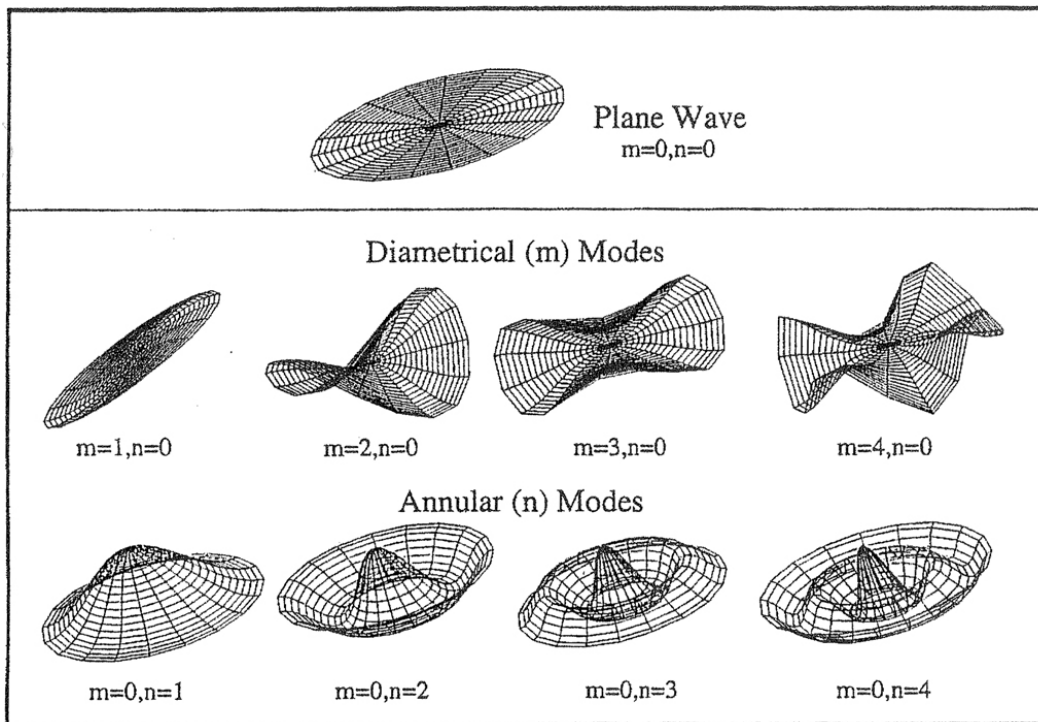


Figure 2: Graphical representation of the reinforcement mechanism of acoustic resonances in pipelines.

Below is an example of acoustic transverse modes for natural gas ($c = 400$ m/s) with a typical pipeline diameter of $D = 250$ mm.

D = 250 mm	m = Number of nodes distributed around the circumference				
n = Number of radial nodes	m = 0	m = 1	m = 2	m = 3	m = 4
n = 0	0 Hz	1,951 Hz	3,575 Hz	5,180 Hz	6,784 Hz
n = 1	937 Hz	2,715 Hz	4,349 Hz	5,964 Hz	7,568 Hz
n = 2	1,553 Hz	3,417 Hz	5,078 Hz	6,707 Hz	8,327 Hz
n = 3	2,140 Hz	4,085 Hz	5,781 Hz	7,431 Hz	9,060 Hz
n = 4	2,709 Hz	4,726 Hz	6,458 Hz	8,128 Hz	9,778 Hz

Table 1: Calculated acoustic transverse mode frequencies (natural gas) with a pipeline diameter of $D = 250$ mm.

The transverse mode frequencies are generally classified as being high frequency (Table 1: Calculated acoustic transverse mode frequencies (natural gas) with a pipeline diameter of $D = 250$ mm.) and often linked to increased noise pollution. These contrast with

the longitudinal, low-frequency acoustic modes of the piping, also known as “longitudinal waves” or “one-dimensional, longitudinal waves”. An example of this is the first acoustic longitudinal mode with dynamic pressure and flow pulsations displayed below in a typical gas pressure regulation plant consisting of an operating and standby pipeline with respective heat exchanger (WT), safety shut-off valves (SAV) and pressure regulator (DR) (Figure 3:

An operating and standby pipeline of a typical gas pressure regulation plant and the dynamic pressure and flow pulsation shown longitudinally in the first acoustic resonance).

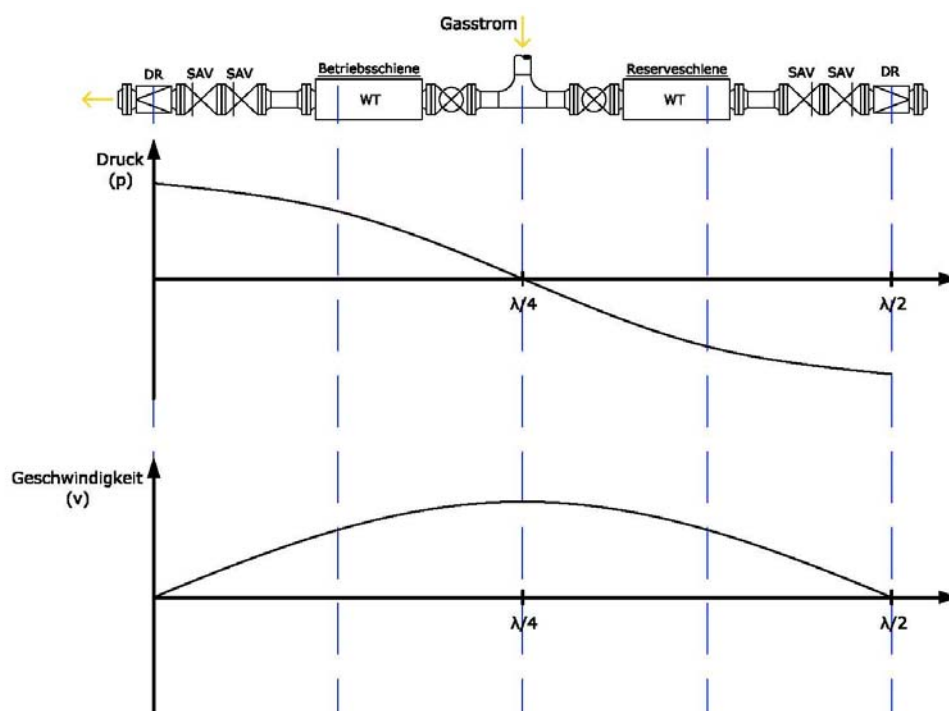


Figure 3: An operating and standby pipeline of a typical gas pressure regulation plant and the dynamic pressure and flow pulsation shown longitudinally in the first acoustic resonance.

Based on the one-dimensional wave equation, the flow velocity v and dynamic pressure p are shown longitudinally in the first acoustic resonance. This results in an acoustically-closed end as a point of reflection where the flow pulsation is zero and the pressure pulsation demonstrates a maximum value both at the pressure regulator of the operating pipeline and at the pressure regulator of the standby pipeline.

The prevalent pressure and flow pulsation depends on the geometric pipeline length between the pressure regulators. Under the same marginal conditions, such as being acoustically

closed, for example, a $\lambda/2$ resonance results as the first fundamental frequency. The resonance frequency can be calculated using equation 1 with the geometric length L between the regulators and the prevalent medium acoustic velocity.

$$f = \frac{c}{\lambda} = \frac{c}{2 \cdot L} \quad (\text{eq. 1})$$

with

c = medium acoustic velocity

λ = wavelength

L = geometric length.

The pressure and flow pulsations linked to this acoustic resonance lead to alternating loads in pipe bends and transverse modifications, and these alternating loads act as a vibration excitation on the pipe structure. Because the externally visible mechanical pipeline vibrations generally occur as low-frequency pipe flexural modes, the results of a measurement conducted with observed longitudinal gas vibrations and mechanical, low-frequency pipe vibrations are analyzed below.

3. Example of a metrological investigation of a GPRM plant

A metrological investigation of a gas pressure regulation and measurement plant was commissioned by its operator due to conspicuous pipe vibrations and conducted by KÖTTER Consulting Engineers. Figure 4: Piping in a GPRM plant with indication of the measurement points (vibration measurement points shown in red, pressure measurement points shown in blue). provides an overview of the piping with the various measurement points used to record the vibration and pressure pulsation situation observed in the GPRM plant.

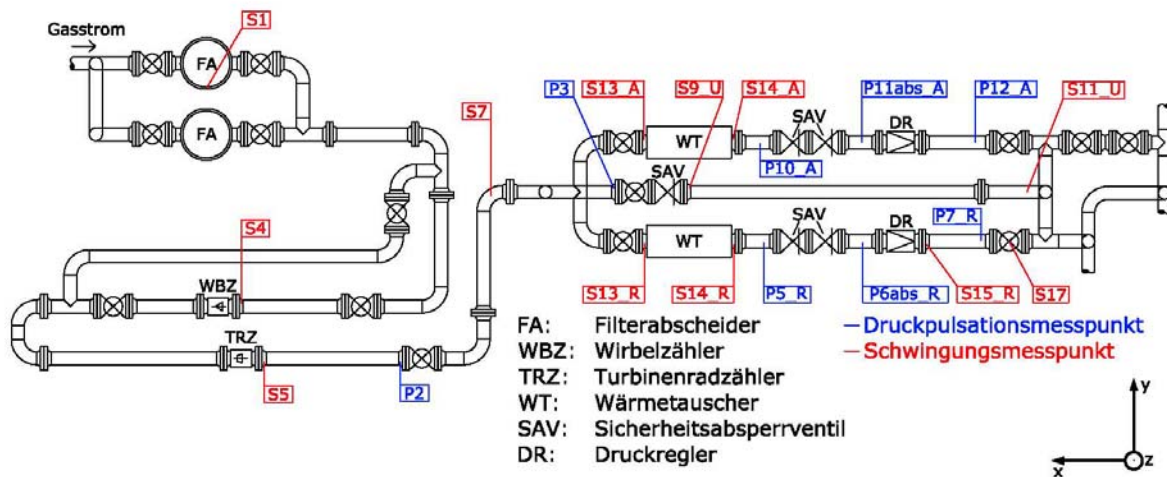


Figure 4: Piping in a GPRM plant with indication of the measurement points (vibration measurement points shown in red, pressure measurement points shown in blue).

Starting with the high-pressure side, gas is passed through the filter separator (FA) followed by the gas quantity measurement using the vortex gas meter (WBZ) and the turbine meter (TRZ) (Figure 4: Piping in a GPRM plant with indication of the measurement points (vibration measurement points shown in red, pressure measurement points shown in blue).). The same procedure is then performed for the low-pressure side, including the operation and standby pipeline with the heat exchangers (WT), the safety shut-off valves (SAV) and the actual pressure regulators (DR).

An excerpt from these measurements is shown below. The maximum vibration rate of approx. 9 mm/s eff. was measured at measurement point S9y_U with a relatively low volume flow of 10,000 Nm³/h within the standby pipe at the point where the heat exchanger's mixing valve was switched from closed (no water passing through the heat exchanger) to fully open (max. water flow through the heat exchanger) (Figure 5: Effective pipeline vibration (measurement point S9y_U), effective pressure pulsation (P6abs_R and P11abs_A) and gas temperature downstream of the control valve (TG1_R) and return water temperature (TW2_R) directly before and after opening the mixing valve of the standby pipeline's heat exchanger (natural gas volume flow 10,000 Nm³/h), 16:04).

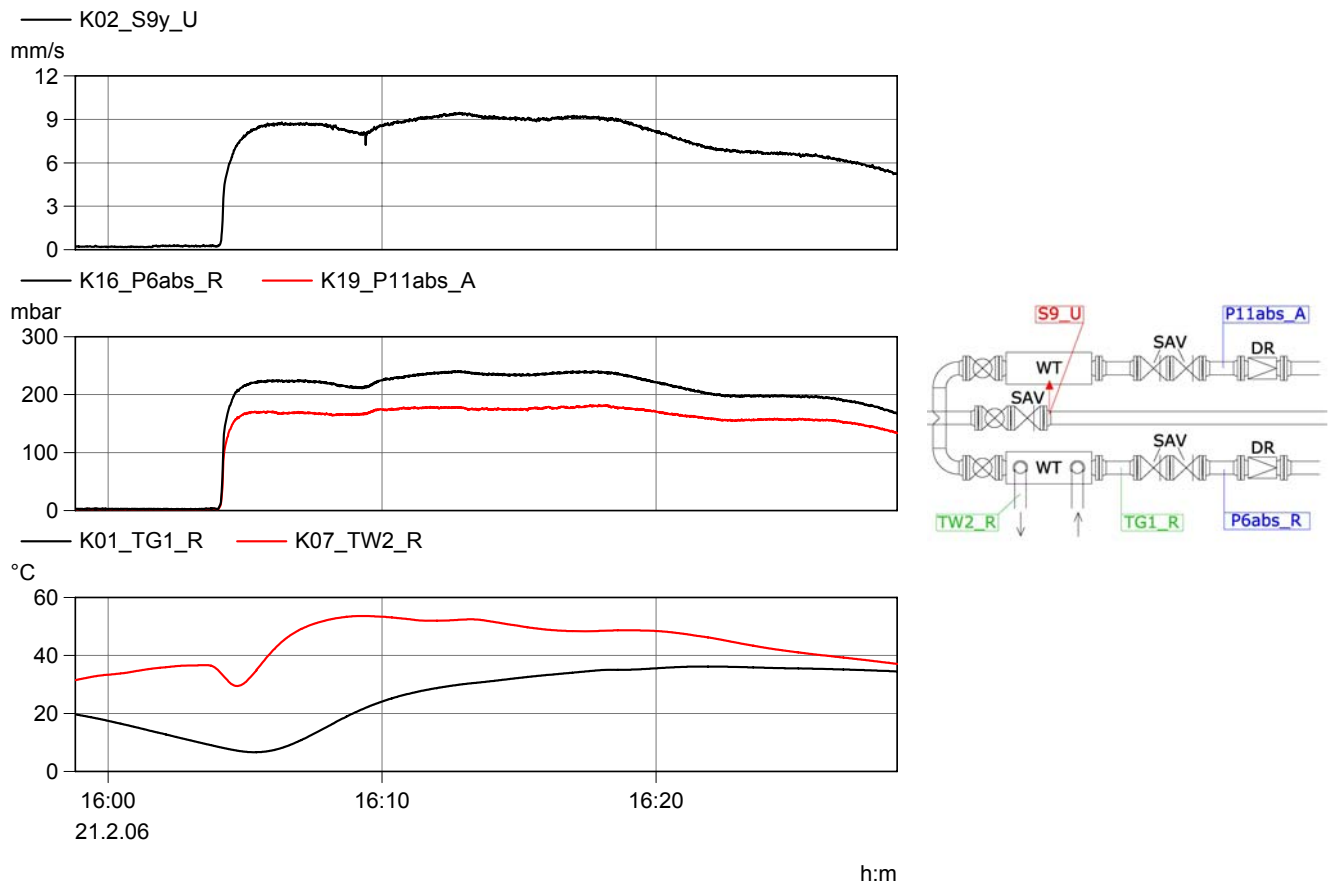


Figure 5: Effective pipeline vibration (measurement point S9y_U), effective pressure pulsation (P6abs_R and P11abs_A) and gas temperature downstream of the control valve (TG1_R) and return water temperature (TW2_R) directly before and after opening the mixing valve of the standby pipeline's heat exchanger (natural gas volume flow 10,000 Nm³/h).

Figure 6: Excerpt from the time-dependent curves of the structure vibrations at measuring point S9y_U and the pressure pulsations at measuring points P6abs_R and P11abs_A (standby pipeline 10,000 Nm³/h, mixing valve of heat exchanger opened after approx. 500 seconds). shows the accompanying time-dependent curves of these signals during a brief period of time.

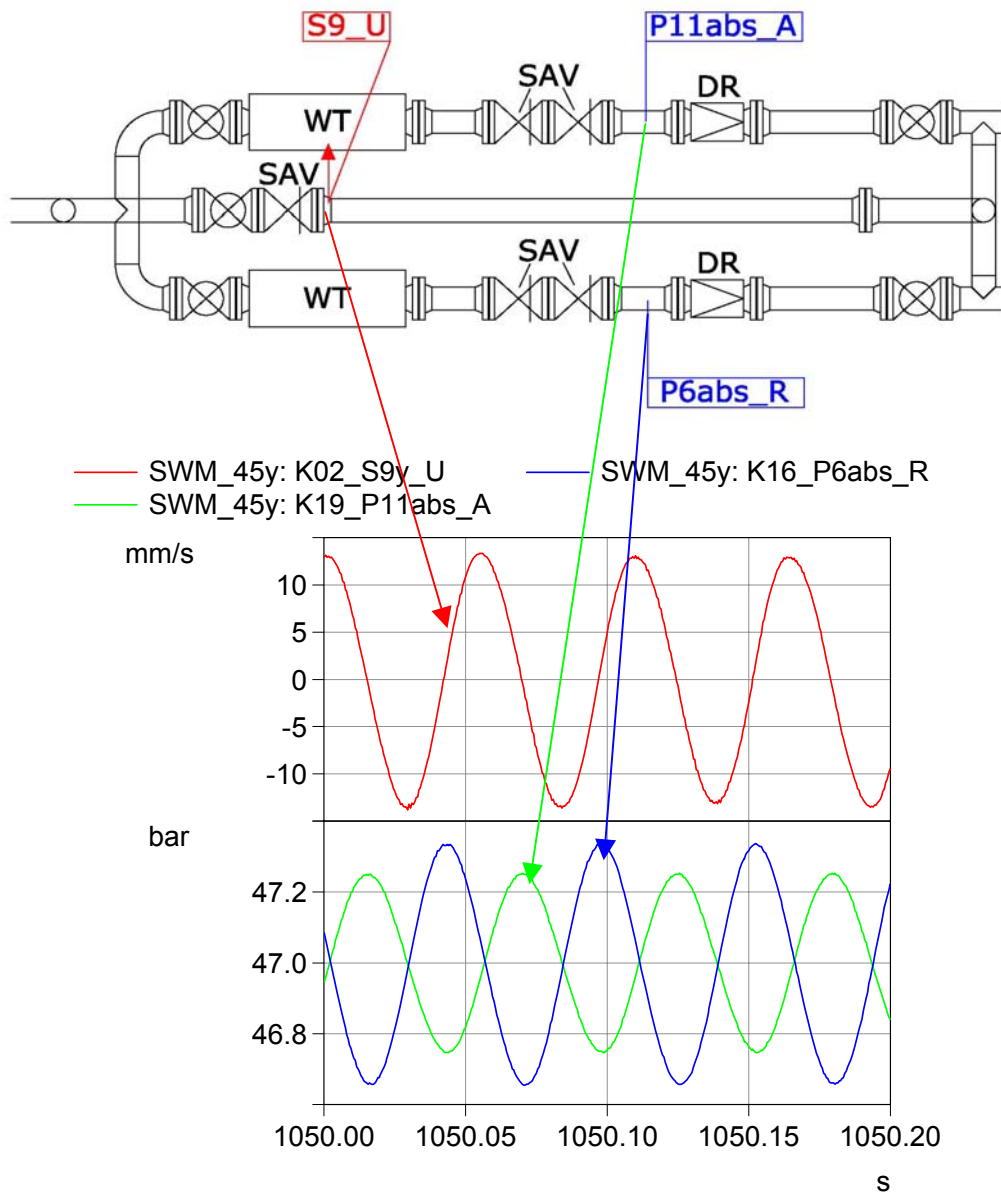


Figure 6: Excerpt from the time-dependent curves of the structure vibrations at measuring point S9y_U and the pressure pulsations at measuring points P6abs_R and P11abs_A (standby pipeline 10,000 Nm³/h, mixing valve of heat exchanger opened after approx. 500 seconds).

It is obvious that the pipe vibrations correlate with the pressure pulsations. The dominant vibrational frequency was measured at 18 Hz. The pressure pulsations within the operation and standby pipeline, which were measured at the same time, were oppositional (Figure 6:

Excerpt from the time-dependent curves of the structure vibrations at measuring point S9y_U and the pressure pulsations at measuring points P6abs_R and P11abs_A (standby pipeline 10,000 Nm³/h, mixing valve of heat exchanger opened after approx. 500 seconds).).

To check this, a simplified analysis of the resonance frequency was performed (according to eq. 1):

$$L = \frac{\lambda}{2} = 11 \text{ m (distance between the pressure regulators)}$$

$$C_{\text{natural gas (40 °C)}} = 400 \frac{\text{m}}{\text{s}}$$

$$f = \frac{c}{\lambda} = \frac{400 \frac{\text{m}}{\text{s}}}{22 \text{ m}} = \underline{\underline{18 \text{ Hz}}}$$

The pressure and flow pulsations linked to this acoustic resonance lead to alternating loads in pipe bends and transverse modifications, and these alternating loads act as a vibration excitation on the pipe structure. Where the inlet temperature of the heat exchanger increased while all other plant conditions, such as the setting of the heat exchanger mixing valve, the gas quantity etc. remained the same, the pressure pulsations and thus the pipe vibrations increased (Figure 7: Effective vibration velocity at measurement point S9y_U (top) and return water inlet temperature of the operation pipe's heat exchanger (TW1_A, bottom) (operation pipe 10,000 Nm³/h).).

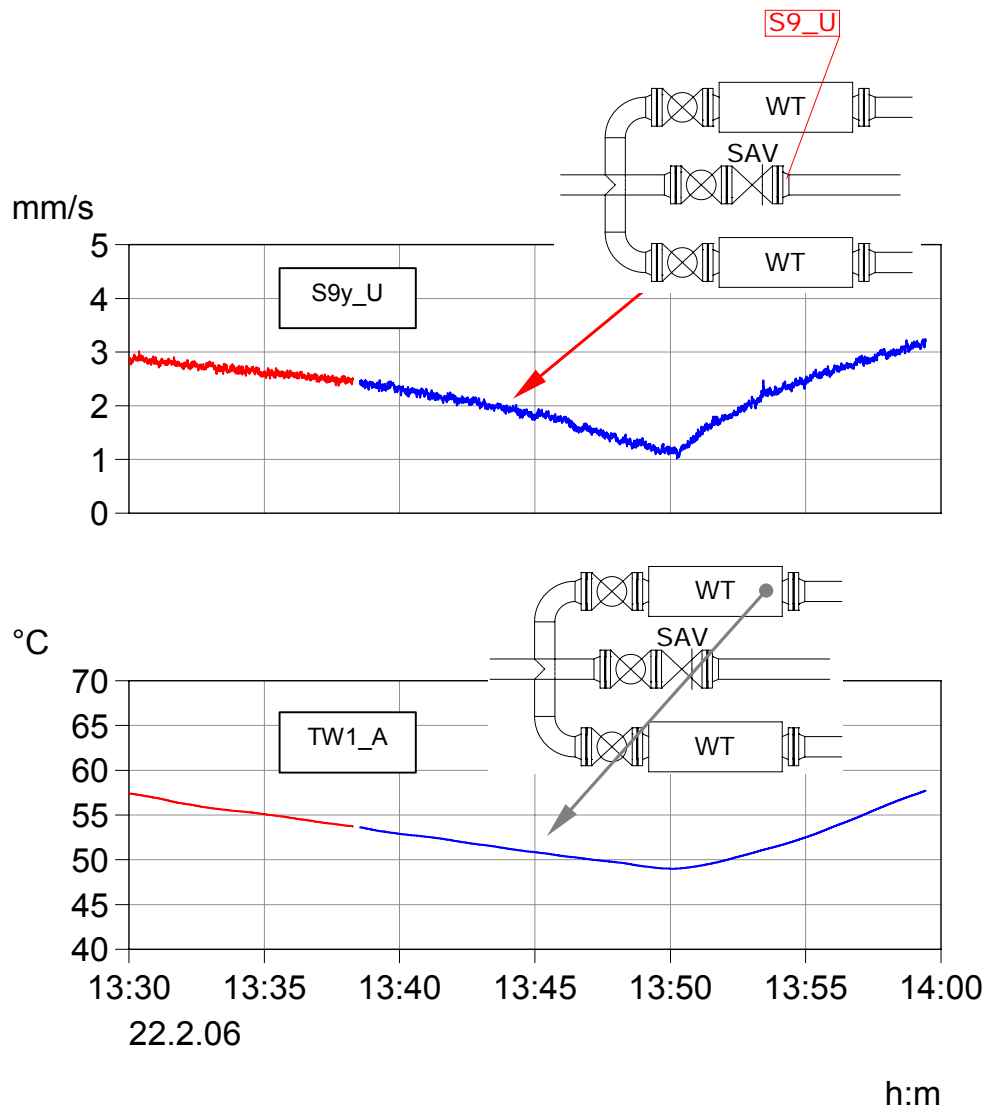


Figure 7: Effective vibration velocity at measurement point S9y_U (top) and return water inlet temperature of the operation pipe's heat exchanger (TW1_A, bottom) (operation pipe 10,000 Nm³/h).

The intensity of the resulting pipe vibrations is defined by the dynamic mechanical characteristics of the structure (natural frequency, damping) along with the level of excitation. These increased pipe vibration characteristics were determined by using a modal hammer to generate force impulse excitation when the plant is not in operation.

The pipe section at measurement point S9y_U thus provides the transfer function illustrated in Figure 8: Transfer function (top) and coherence (bottom) between the pulse excitation and the vibration velocity at measurement point S9y_U. that occurs between the exciting force (modal hammer) and the resulting vibration intensity. This pipe section is shown to

have a distinctive natural structural-mechanical frequency at 19 Hz and approx. 22 Hz respectively.

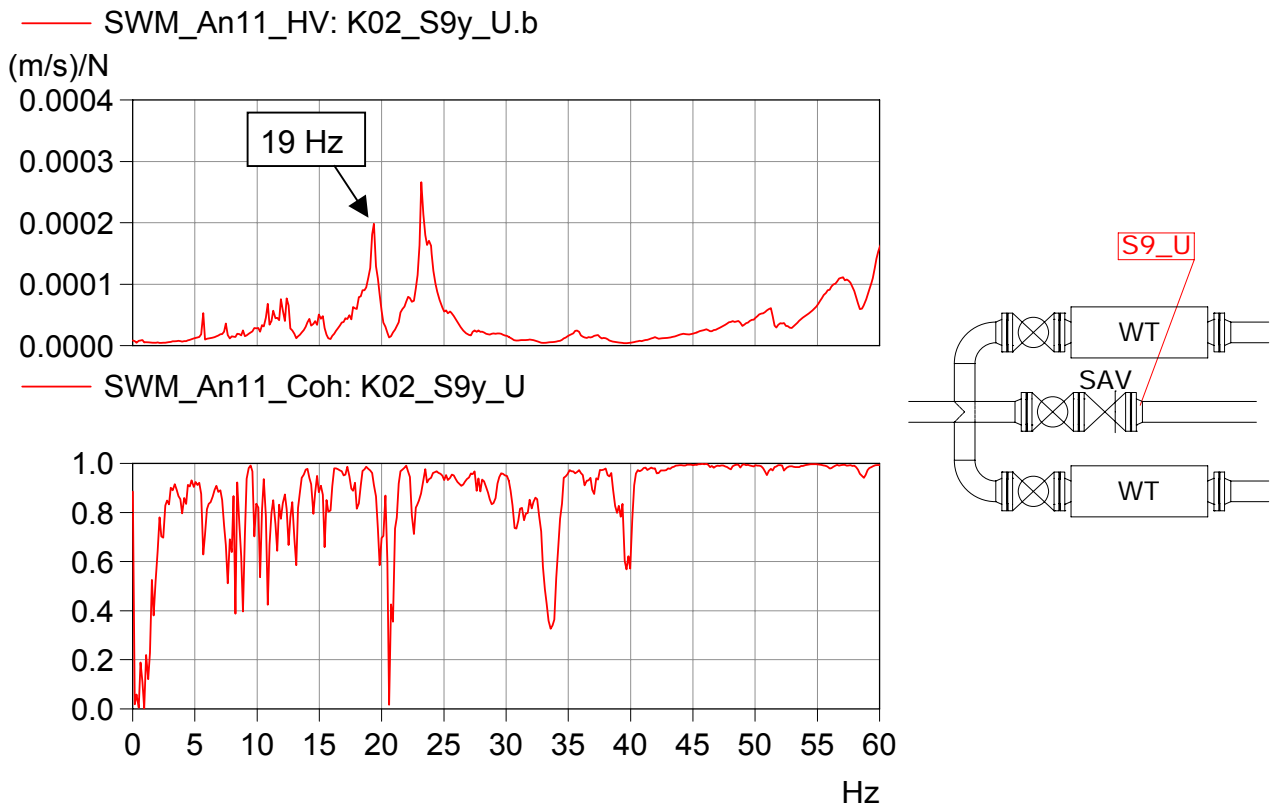


Figure 8: Transfer function (top) and coherence (bottom) between the pulse excitation and the vibration velocity at measurement point S9y_U.

Around measurement point S9y_U the 18-Hz vibrations excited by pressure pulsations / acoustic resonance are increased on account of a mechanical natural frequency within a similar range (19 Hz). It is therefore to be expected that, when compared to the measured situation, the acoustic resonance frequency will shift from 18 Hz to 19 Hz. This in turn leads to stronger pipeline vibrations, meaning that the permissible orientation values in [2] will inevitably be exceeded. Such acoustic resonance frequency shifts to 19 Hz are caused by a 5% increase in acoustic velocity. For this to happen, the gas temperature as measured on the Kelvin scale has to increase by around 11%.

The described acoustic resonance within the pipeline between the control valves of the operation and standby pipe also leads to a pulsating flow around the flow meters. This unsteady flow influences the gas quantity meters. In cases of pulsating flow, turbine meters principally exhibit an excessive flow compared to the actual volume flow. With vortex gas

meters, various effects occur that can lead to incorrect readings that may be either too high or too low. Previous experience has shown that vortex gas meters generally tend to return readings that are too low in the case of a pulsating flow.

The influence of the pulsating flow on the turbine meters can in this case be observed in the form of the high-frequency pulse signal spectrum of the impeller. With a steady flow, the turbine meter's impeller spins at a constant peripheral velocity. In the high-frequency pulse signal's color spectrogram there is a corresponding blade pass frequency amplitude (number of revolutions x number of blades) (Figure 9: Color spectrogram of the turbine meter's high-frequency pulse signal and the effective pressure pulsation curve at measurement point P2 (standby pipe 10,000 Nm³/h, mixing valve of heat exchanger opened after approx. 500 seconds) , 400 – 520 s). With a pulsating flow (low to medium pulsation frequency), the impeller's peripheral velocity also pulsates. Correspondingly, the impeller spins slower or faster depending on the change in pulsation frequency. In the high-frequency pulse signal's color spectrogram this frequency modulation is visible in the form of side bands next to the carrier frequency (blade pass frequency). The distance of the side bands from the carrier frequency corresponds to the pulsation frequency (18 Hz in this case) (Figure 9: Color spectrogram of the turbine meter's high-frequency pulse signal and the effective pressure pulsation curve at measurement point P2 (standby pipe 10,000 Nm³/h, mixing valve of heat exchanger opened after approx. 500 seconds) , 520 – 1,000 s).

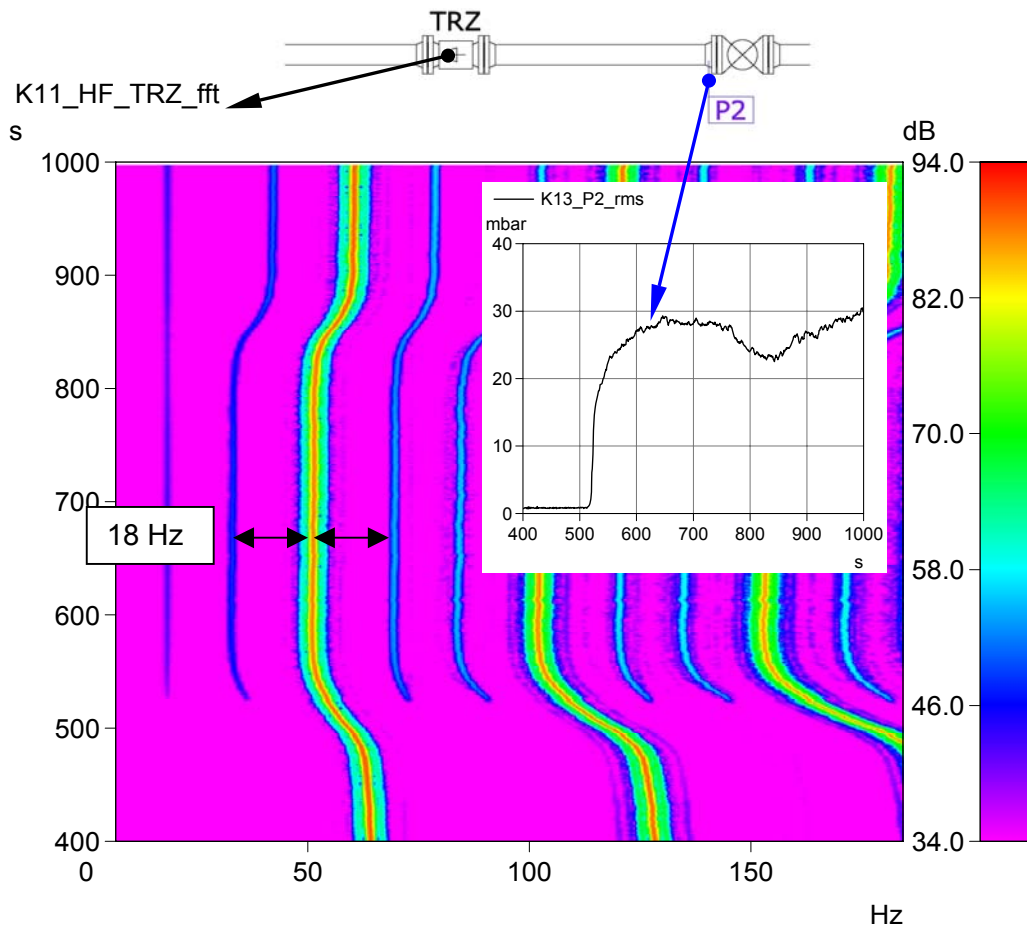


Figure 9: Color spectrogram of the turbine meter's high-frequency pulse signal and the effective pressure pulsation curve at measurement point P2 (standby pipe 10,000 Nm³/h, mixing valve of heat exchanger opened after approx. 500 seconds)

The pulsating flow's influence on the vortex gas meter is depicted in Figure 10: Effective pressure pulsation at measurement point P2 (top), operation volume flow of the turbine meter (middle) and pulse frequency of the vortex gas meter (bottom) over time (standby pipe 10,000 Nm³/h, mixing valve of the heat exchanger opened after approx. 520 seconds). . As a result of the unsteady flow, the rigid body's vortices periodically separate in a somewhat unstable manner. The vortex gas meter's measurement accuracy therefore decreases and, in this case, it leads to the meter failing (T = 520 s) with periodic vortex separation no longer being registered. From around 560 s onwards, the depicted vortex separation frequency is no longer proportional to the volume flow but simply the normal pulsation frequency (18 Hz) or about half thereof (9 Hz).

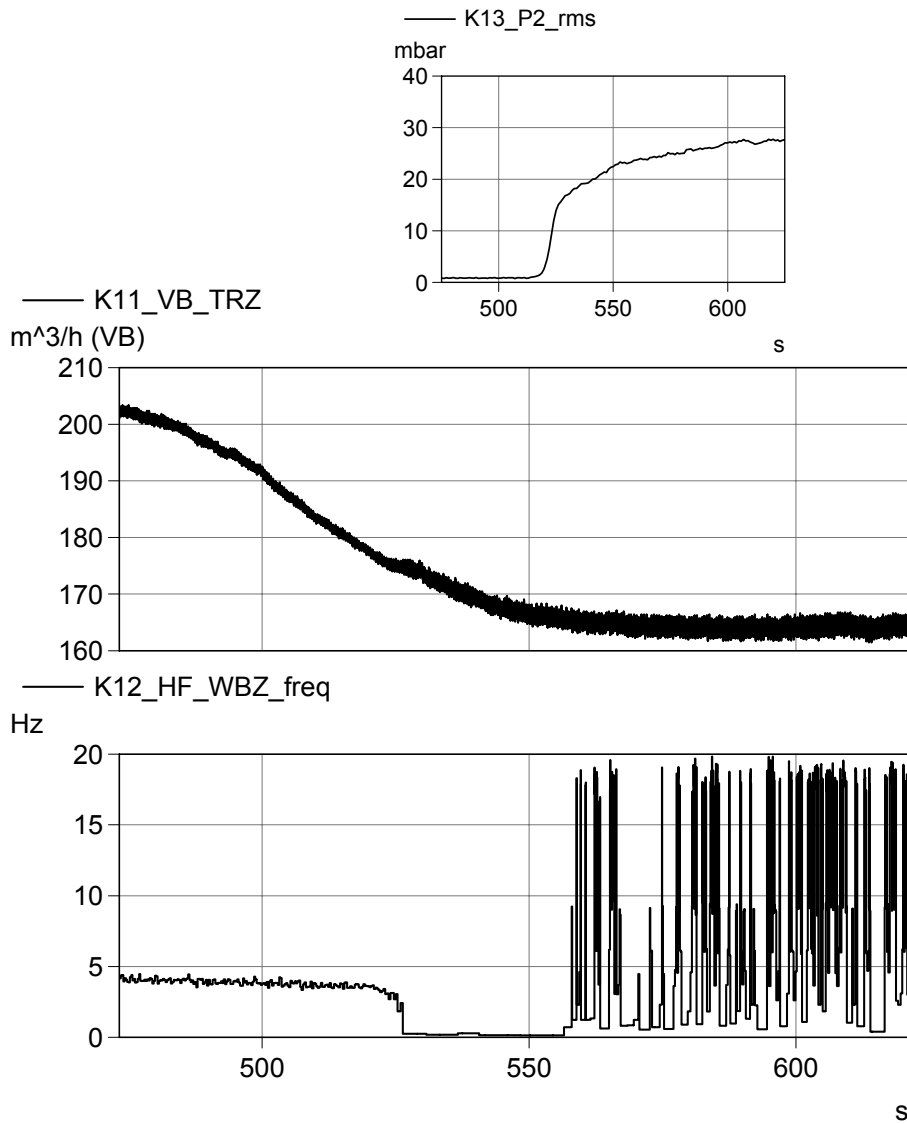


Figure 10: Effective pressure pulsation at measurement point P2 (top), operation volume flow of the turbine meter (middle) and pulse frequency of the vortex gas meter (bottom) over time (standby pipe 10,000 Nm^3/h , mixing valve of the heat exchanger opened after approx. 520 seconds).

Due to the described circumstances, reliable volume flow measurements below 14,000 Nm^3/h could no longer be ensured. The link ascertained between the gas quantity measurement influence and the acoustic resonance is illustrated in Figure 11: Effective pressure pulsations at measuring point P6abs and timing error E across the operation volume flow for the KCE measurements (red and blue symbols) and in keeping with the

inspection reports (yellow symbols). as timing error E (eq. 2) of the meters connected in series.

$$E = \frac{V_{B,WBZ} - V_{B,TRZ}}{V_{B,TRZ}} \cdot 100 [\%] \quad (\text{eq. 2})$$

with

E = timing error in percent

$V_{B,TRZ}$... = operation volume flow of the turbine meter

$V_{B,WBZ}$... = operation volume flow of the vortex gas meter

The red and blue symbols are based on readings taken by KCE. The yellow symbols represent the results of the comparative meter measurements for the inspection carried out on behalf of the operator over the course of the last five years.

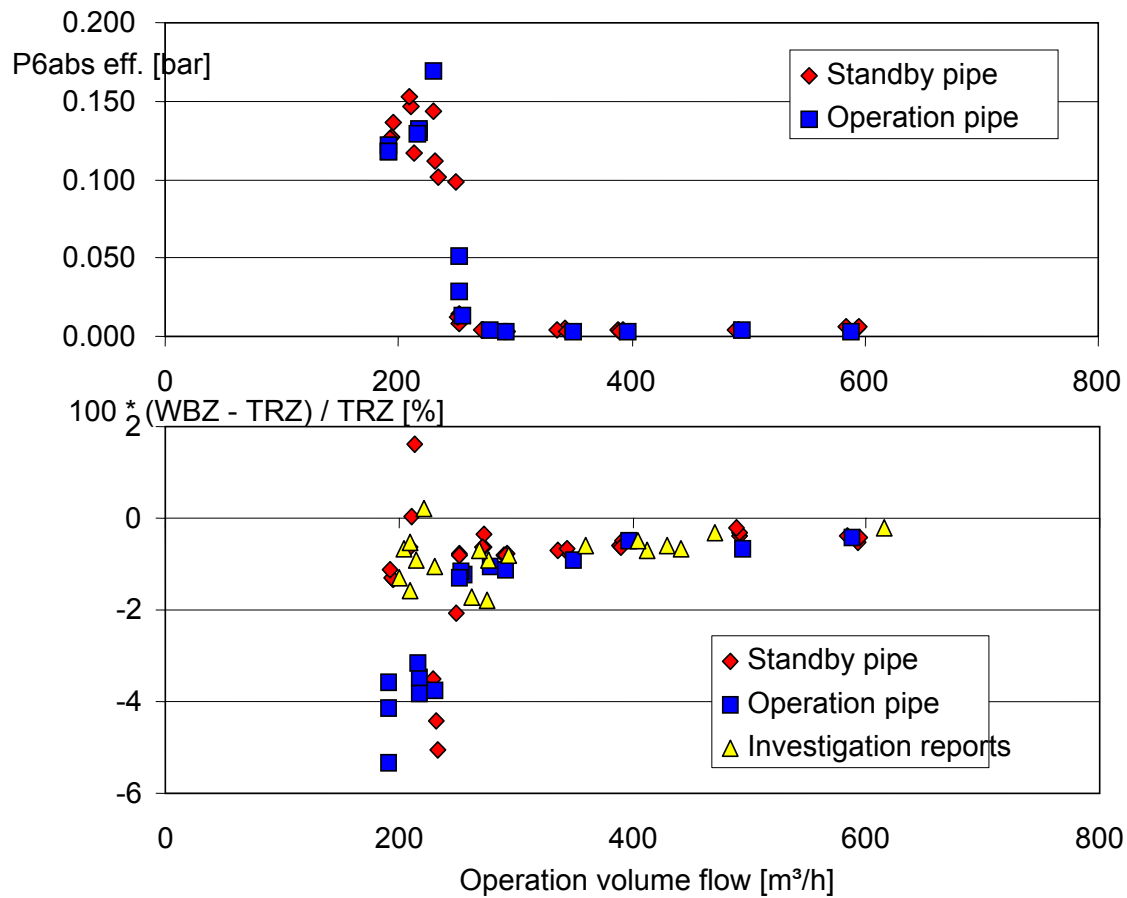


Figure 11: Effective pressure pulsations at measuring point P6abs and timing error E across the operation volume flow for the KCE measurements (red and blue symbols) and in keeping with the inspection reports (yellow symbols).

When compared to the mathematical measurement inaccuracy, the pulsation range of timing error E is much higher for the KCE readings and the inspection report results, especially below 250 m³/h (V_B). In terms of the KCE readings, this increased pulsation range correlates with the formation of acoustic resonance, whose existence can be derived from the effective value of the pressure pulsations at measurement point P6abs.

Conclusion of the metrological investigation

The investigated GPRM plant demonstrated an acoustic resonance and therefore excited pipeline vibrations coupled with increased gas quantity meter timing errors during operation with low volume flow. The pressure pulsations causing this can be increased if heat transfer (to the gas flow) takes place via the heat exchanger. The cause of this behavior was

previously unknown among GPRM plants. Irrespective of this, the phenomenon has already been observed among a number of gas transfer and regulation plants where the described dependencies on heat transfer in the heat exchanger and the magnitude of the acoustic resonance / pipeline vibrations were comparable and reproducible.

4. Experiment using a heat exchanger to cause vibration excitation

Energy technology experience has shown that combustion processes interact with acoustic phenomena in different ways. Combustion vibrations can lead to feedback between heat transfer and plant acoustics. The self-amplifying characteristic, also known as self-exciting thermoacoustic instability, is indicative of this type of feedback. This phenomenon of thermal expansion interacting with acoustics was discovered by Higgins in 1777 [3]. He lit a hydrogen flame which, depending on the position of the flame within a glass tube, produced a highly audible tone. In the mid 19th century, Rijke used a “Rijke tube” to demonstrate a fundamental way of understanding self-exciting, thermoacoustic vibration [4].

Figure 12: Photo showing the experiment design to test thermodynamic instability. and

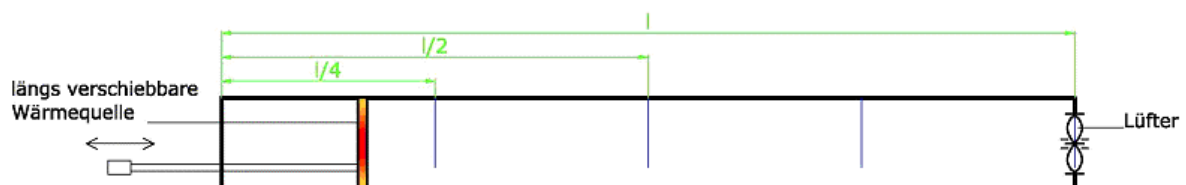


Figure 13: Schematic diagram with positioning information to prove thermodynamic instability. show an experiment designed in a similar way to a parallel operation and standby pipe with a heat source comparable to a heat exchanger, which can be moved longitudinally within the pipe. The pipe has been replaced with a transparent tube made of glass. A fan is fitted at the end of the tube to simulate variations in volume flow. The heat source, which can be moved longitudinally, consists of a simple wire mesh powered by a variable electrical source so that the wire can be controlled directly, like an active heat source.

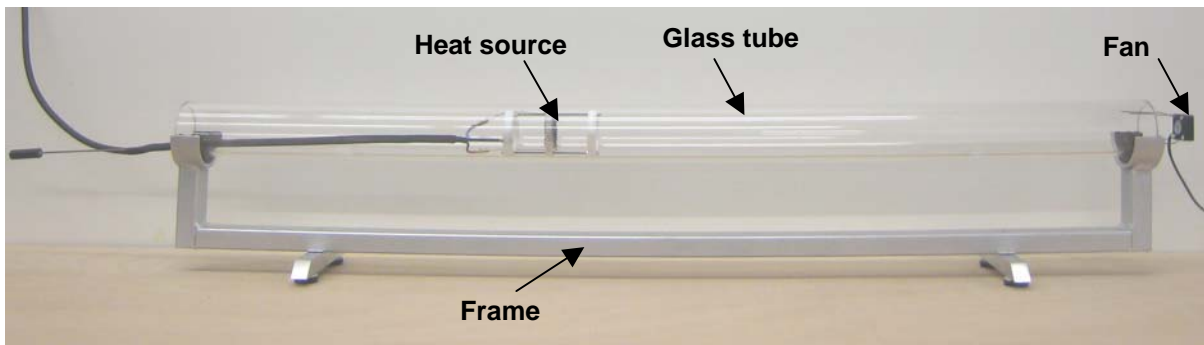


Figure 12: Photo showing the experiment design to test thermodynamic instability.

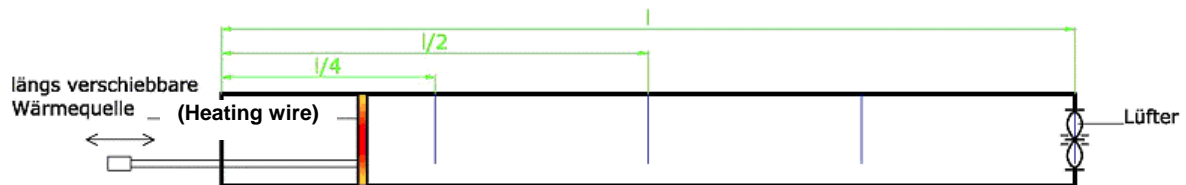


Figure 13: Schematic diagram with positioning information to prove thermodynamic instability.

The marginal conditions of both ends of the acoustically open glass tube lead to the formation of a potential acoustic resonance with a wavelength of $\lambda/2$. As thermoacoustic instability publications have shown, the position of the heat source and the intensity of the volume flow have a crucial influence on the formation of instability, so the decision was made to have both factors variable during the experiment.

In order to test the method, the fan was set to produce a relatively low volume flow. The heating wire is then heated by increasing the flow of electricity. The air drawn in by the fan then warms up a little. Heat transfer to the medium (air) then occurs at the heating wire. Minor flow pulsations and influence due to the heating wire's boundary layer lead to pulsations in the transferred thermal output. These, combined with local thermal air expansion, in turn lead to pressure pulsations that propagate in the tube as waves and are partially reflected at the ends of the glass tube (see Figure 14: The thermoacoustic instability feedback principle).

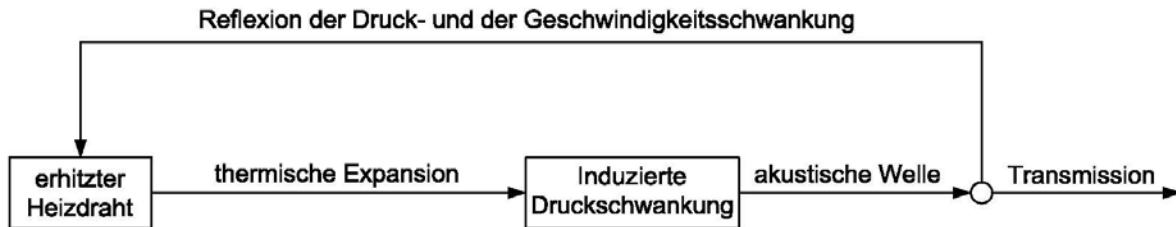


Figure 14: The thermoacoustic instability feedback principle

Under certain conditions this reflection can lead to feedback, meaning that pressure and flow pulsations are again induced on account of the reflected flow pulsation at the heating wire. By changing the position of the heating wire within the glass tube, the phase relation critical to acoustic instability varies between pressure pulsation p and heat quantity pulsation q' .

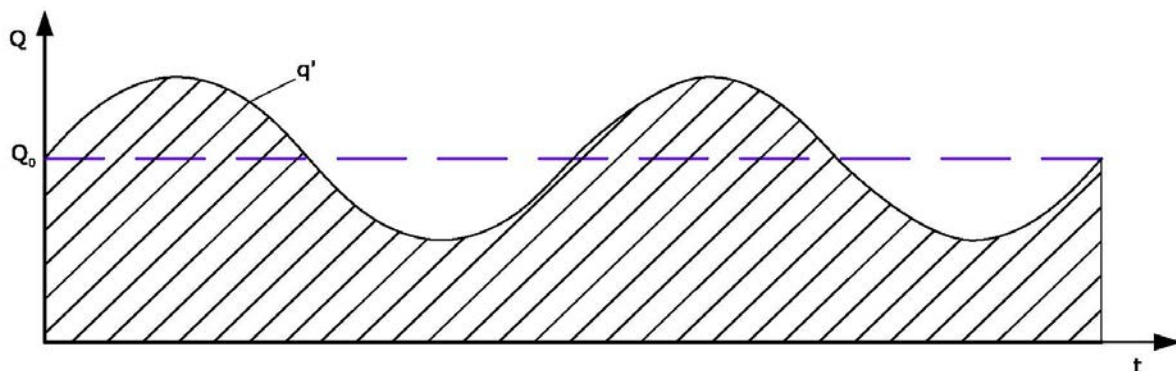


Figure 15: Heat quantity curve with constant heat quantity Q_0 and heat quantity pulsation q' .

If the phase relation between pressure pulsation and heat quantity pulsation changes in such a way that the increasing pressure coincides with an increase in heat, then a reciprocal build-up occurs which in turn leads to self-excited gas vibrations in the form of acoustic resonance. The link between the unsteady heat quantity pulsation and acoustic pressure pulsation described in the equation below (eq. 3) represents a sufficient criterion for the occurrence of thermoacoustic instability.

$$R = \int_t^{t+T} p(t)q'(t)dt \quad (\text{eq. 3}),$$

This is also known as Rayleigh Integral or Rayleigh Index R. The heat quantity pulsation q' is proportional to the acoustic flow pulsation v with phase delay δ

$$q'(t) \sim v(t - \delta).$$

Figure 16: Qualitative representation of acoustic pressure pulsation p , heat quantity pulsation q' depending on the heat source position and the Rayleigh Index R as conditions within the glass tube. is a qualitative representation of p , v and Rayleigh Index R for each possible heat source position within the glass tube.

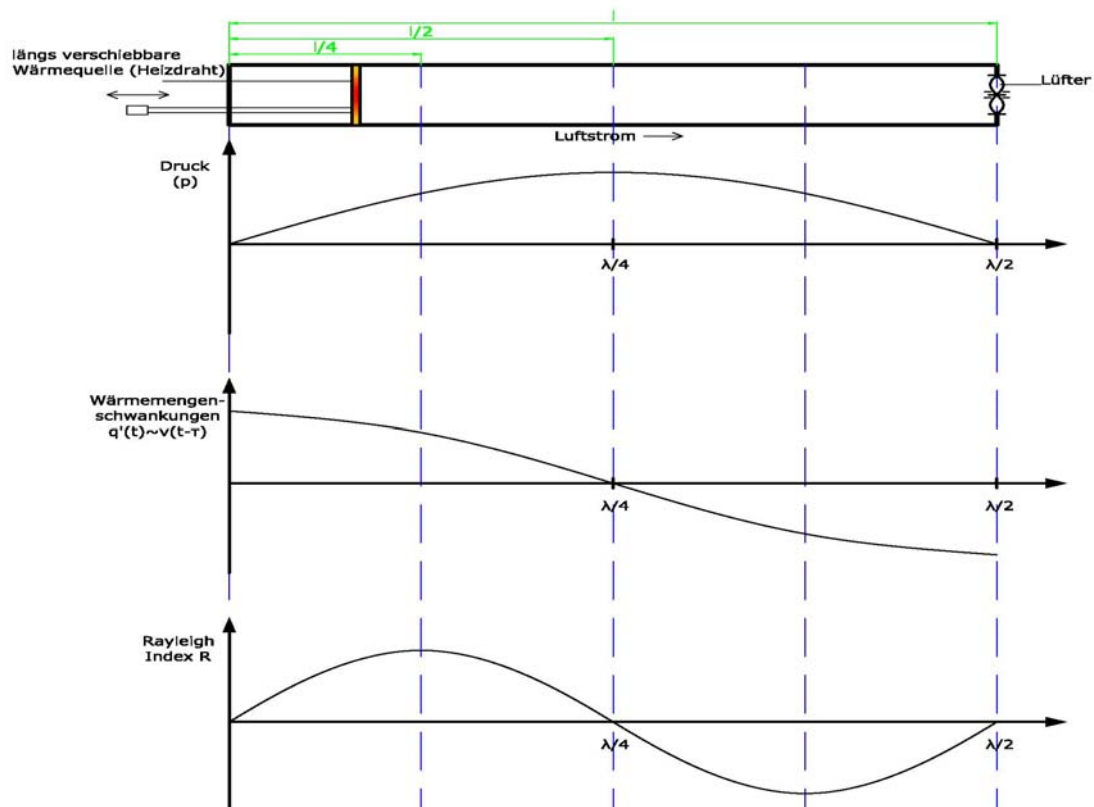


Figure 16: Qualitative representation of acoustic pressure pulsation p , heat quantity pulsation q' depending on the heat source position and the Rayleigh Index R as conditions within the glass tube.

The Rayleigh Index describes the necessary yet insufficient condition required to generate self-exciting thermoacoustic vibrations. Depending on the algebraic sign preceding the Rayleigh Index, there is either a damping or a build-up of gas vibration, which in turn leads to acoustic resonance.

$R < 0$ Acoustic resonance damping

$R = 0$ Neutral behavior

$R > 0$ Acoustic resonance build-up

In order to prove this link by means of experiment, the fan is initially set to a relatively low volume flow and the heat source positioned at the end of the glass tube. The heating wire is heated, and the temperature of the air drawn into and through the glass tube rises noticeably. No other changes are observed.

Now the heating wire is moved along the glass tube. At point $l/4$ there is a clearly audible build-up of acoustic resonance with a monofrequent tone of approx. 180 Hz. When the heating wire is moved further along the glass tube, the intensity of the tone drops rapidly. At all other positions between this point and the end of the glass tube, there is no further acoustic resonance build-up. When the heating wire is moved back to position $l/4$, the tone is again audible. In addition, the pressure pulsation amplitude can also be increased by increasing the heating wire temperature, as is the case when measuring the heat exchanger of the GPRM plant.

5. Transfer to and analysis of previous results on a GPRM plant

In order to perform a direct comparison of the measurements,

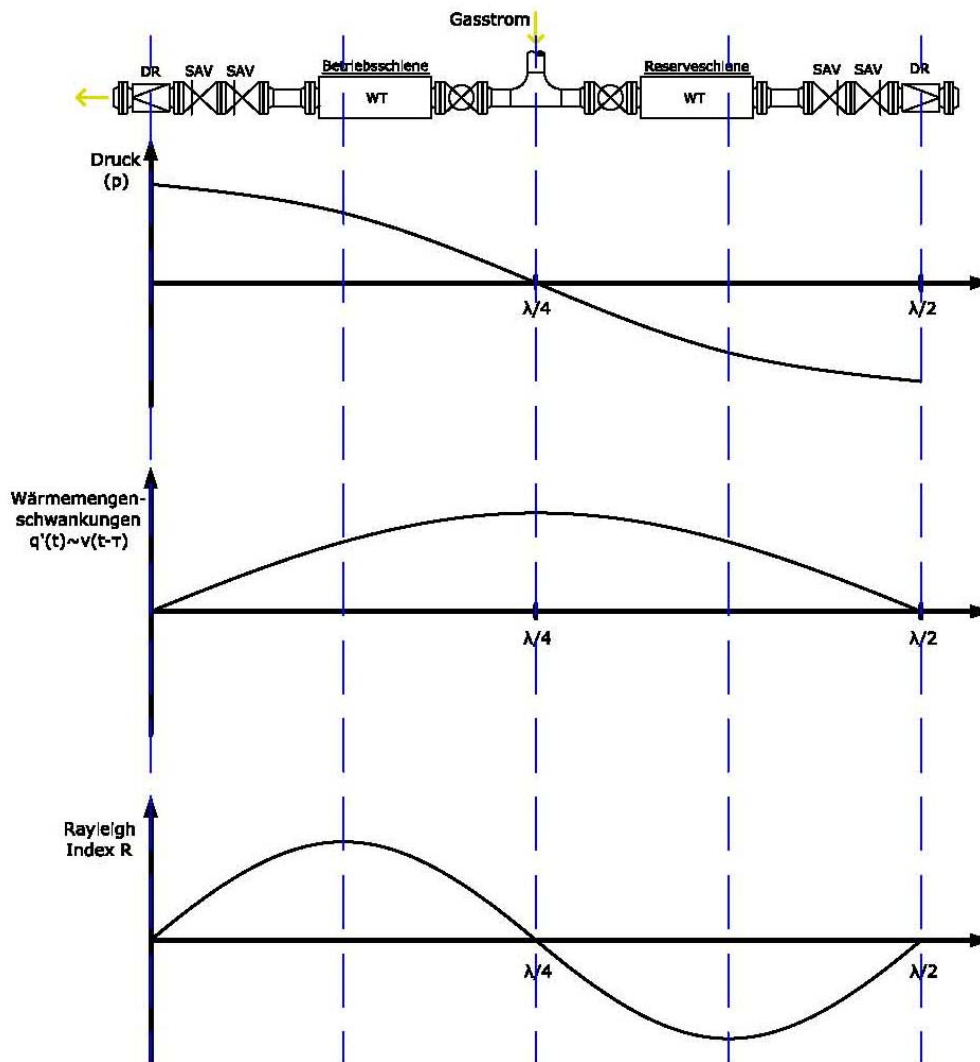


Figure 17: Qualitative representation of the acoustic pressure pulsation of heat quantity pulsation q' in dependence on the heat source position and the Rayleigh Index R as conditions for a GPRM plant. shows the Rayleigh Index curve during the typical operation of a GPRM plant's operation and standby pipeline.

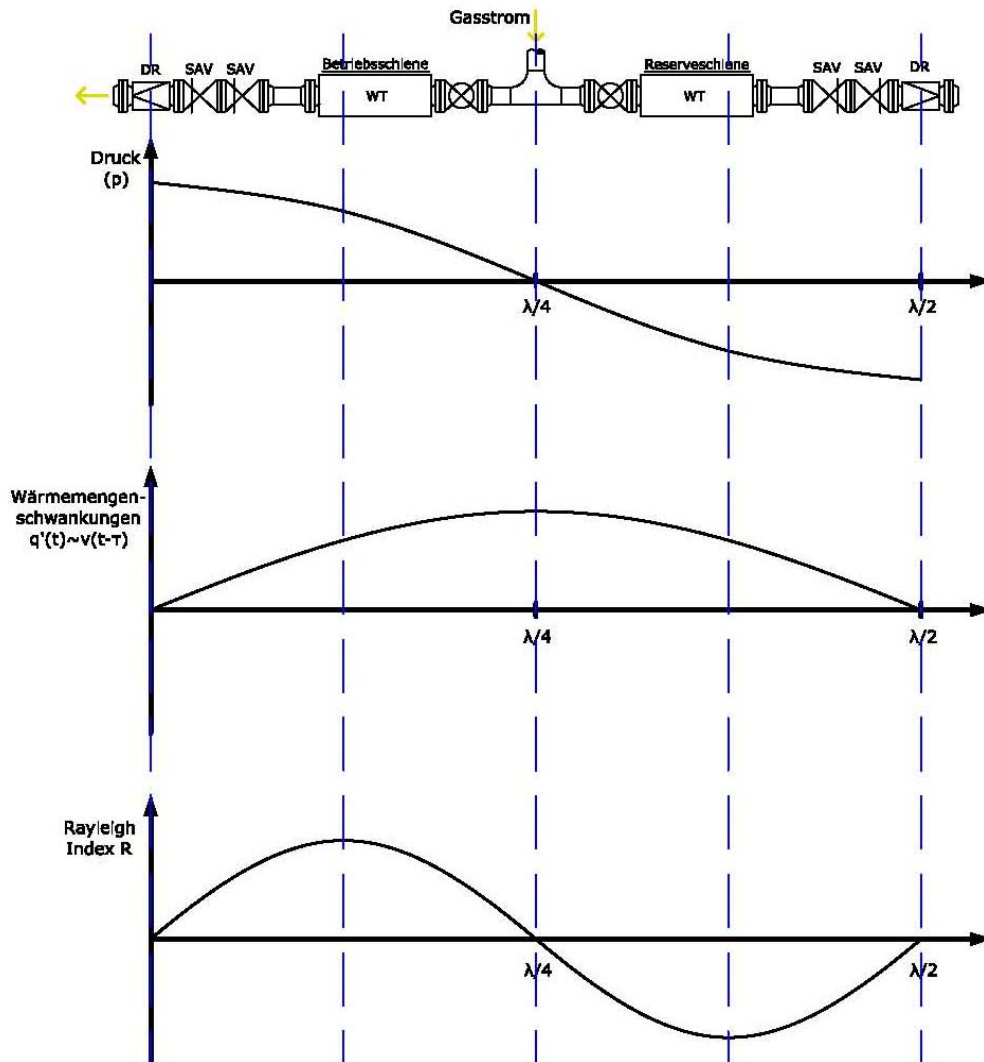
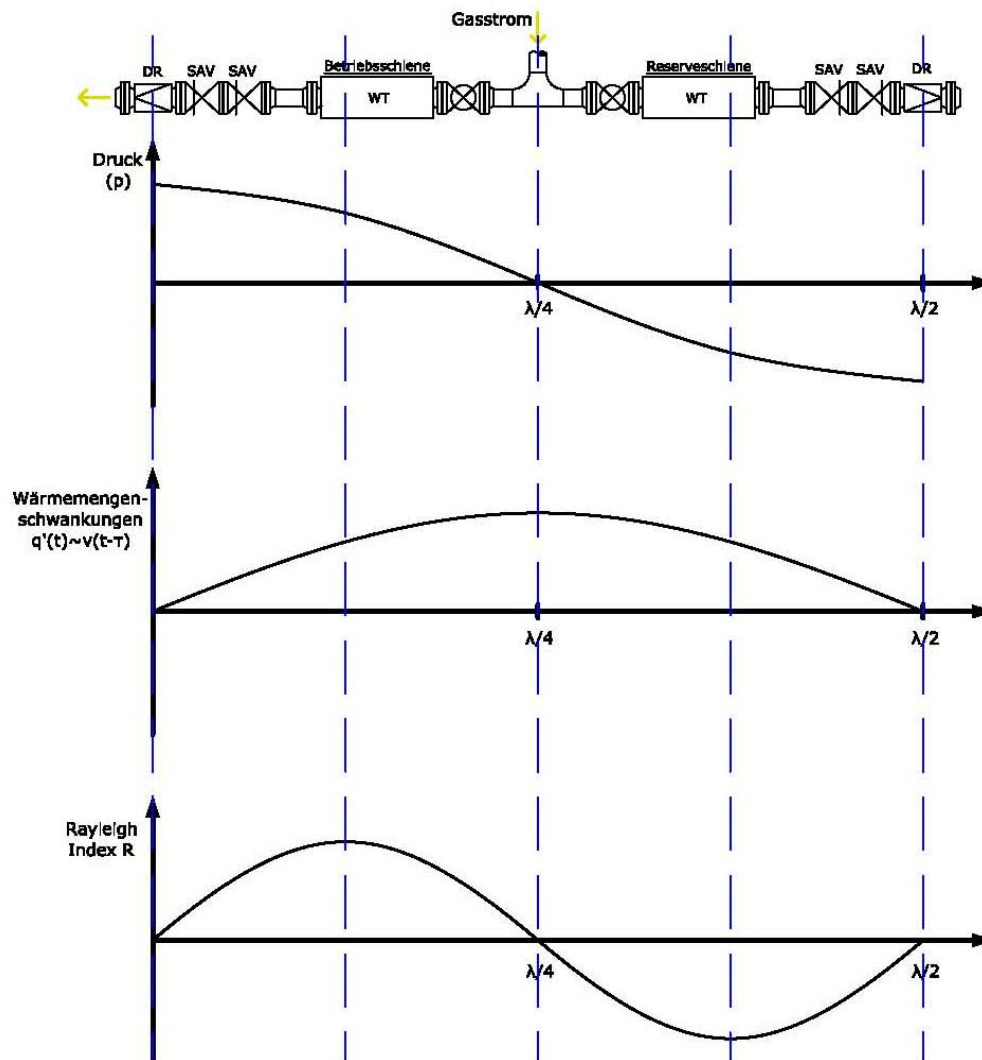


Figure 17: Qualitative representation of the acoustic pressure pulsation of heat quantity pulsation q' in dependence on the heat source position and the Rayleigh Index R as conditions for a GPRM plant.

The Rayleigh Index curve confirms that the location of the potential thermoacoustic instability build-up and the actual installation position of the heat exchanger within a GPRM plant can definitely coincide. This geometric compatibility was present in the plant under investigation.

However, the position of the second heat exchanger in the standby pipeline requires

discussion. The Rayleigh Index



(

Figure 17: Qualitative representation of the acoustic pressure pulsation of heat quantity pulsation q' in dependence on the heat source position and the Rayleigh Index R as conditions for a GPRM plant.) curvet demonstrates major damping of potential acoustic resonance. This does not however take into account that there is no flow in the closed-off standby pipe and thus no fundamental heat transport – a basic requirement for thermoacoustic instability.

Also to be taken into account is the fact that the Rayleigh Index represents a necessary yet insufficient condition required to generate self-exciting thermoacoustic vibrations. To ensure that acoustic resonance occurs when this criterion is fulfilled, the energy supplied in the form

of heat has to be greater than the energy loss that occurs as a result of dissipation and radiation.

6. Potential reduction measures

There are in principle various ways of reducing or avoiding the occurrence of thermoacoustic instabilities. The first consideration is whether the GPRM plant is a new one currently under development or an existing one.

With new plants, the build-up of self-exciting vibrations can be prevented by applying current knowledge and positioning the heat exchanger in a specific position to be determined by means of a pulsation study. Alternatively, positions for the specific use of damping attenuators in the gas flow (e.g. pulsation damper plates) can be calculated and designed for practical deployment.

In the case of existing GPRM plants with highly fluctuating requirements in terms of volume flow and pressure difference, we recommend a theoretical investigation of potential build-up options of thermoacoustic instabilities. If potential indications of self-exciting vibrations become apparent during such a pulsation investigation, the acoustics and structural dynamics should be measured and recorded for selected operating positions. The knowledge obtained from this investigation can be used to plan and deploy structural and mechanical measures (e.g. additional pipeline supports) or acoustic measures (e.g. pulsation damper plates).

7. Conclusion and outlook

For the first time, a metrological investigation of an existing GPRM plant and an adapted experiment were able to prove that thermoacoustic instabilities cause increased pressure pulsations in dependence on the position of the heat exchanger. These pulsations also cause the gas quantity meters to behave erroneously. Serious mechanical damage [1] may be incurred if the pressure pulsation frequency matches the natural structural frequency of the pipeline plant.

In order to prevent this from happening, various options and recommendations are demonstrated both for existing and new plants. These results are pursuant to the latest knowledge and developments. Other questions regarding thermoacoustic instability, especially pertaining to numerical considerations, are currently being investigated together with the Department of Fluid Technology at the Technische Universität (Technical University) in Dortmund.

8. Literature

- [1] *Hightech-Erneuerung der Gasübernahmestation Bernburg-Peißen, energie/wasser-praxis, 2/2005* (High-tech renewal of the gas off-take plant in Bernburg-Peißen, energie/wasser-praxis, 2/2005)
- [2] *VDI-Richtlinie 3842, Schwingungen in Rohrleitungssystemen, Juni 2004* (VDI - Association of German Engineers - Guidelines 3842, Vibrations in piping systems, June 2004)
- [3] B. Higgins. On the sound produced by a current of hydrogen passing through a tube. *Journal of natural philosophy, chemistry and the arts*, 1:129-131, 1802.
- [4] P. L. Rijke. *Notiz über eine neue Art, die in einer an beiden Enden offenen Röhre enthaltene Luft in Schwingungen zu versetzen.* (Note regarding a new way of generating vibrations in the air contained in a tube open at both ends.) *Annalen der Physik und Chemie*, 107:339-343, 1859.